EECS C106B / 206B Robotic Manipulation and Interaction **Spring 2021**

Lecture 25: Modeling and Dynamics of Legged Robots

Scribes: Neelay Junnarkar

25.1 Introduction

25.1.1 Motivation

Why legs?

- Mobility: See Figure 25.1.
- Prosthetics
- Service robots
- Transportation

Figure 25.1: Goats licking salt on cliffsides. Animals are able to use their legs beyond the capabilities of current robots to climb difficult terrain.

25.1.2 Goals

Common goals of legged robot research and design include:

- Running (fast)
- Safety critical walking (stepping stones)

25.1.3 Challenges

Challenges faced in legged robot design include:

- Multiple degrees freedom
- High degree of underactuation
- Nonlinear and hybrid models
- Controllers for producing stable periodic orbits
- Periodic versus static equilibria
- Robustness to (unknown) rugged terrain

25.2 History

The first 'legged' robots were walking horse mechanisms designed in the late 1800s. These were powered by pedals, much like bicycles. In the 1950s and 1960s, walking machines were designed. General Electic's 1965 "Walking Truck" (see Figure 25.2) was a hydraulically actuated quadruped controlled by a human driver.

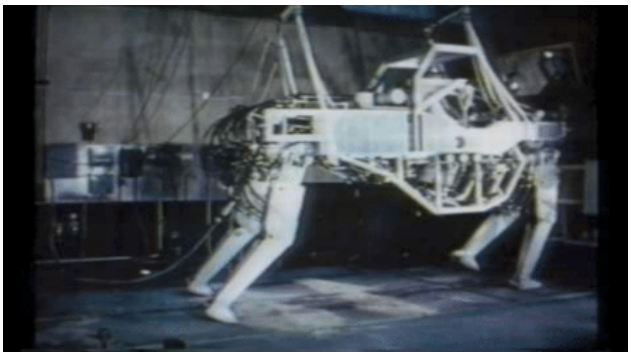

Figure 25.2: General Electric's 1965 Walking Truck

In the 1980s and '90s, Raibert's Leg Lab at CMU and later MIT designed hopping robots, bipedal, and quadrupedal robots. In 2000, Honda's ASIMO service walker robot was released, an example of a zero moment point walker. A DARPA walking robotics challenge in 2012 demonstrated additional need for robustness.

In the past few decades, there have been huge advances in legged robot technology, with robots such as the well known ATLAS from Boston Dynamics (founded by Raibert of Raibert Lab).

25.3 Cassie on Hovershoes

While legged robots are advantageous on rough terrain compared to wheels, there are still many flat surfaces (especially in human environments) where legs are less efficient compared to wheels. Motivated by scenarios such as humans often switching between different modes of transport (e.g. skateboard when possible, walk

Figure 25.3: Boston Dynamic's ATLAS robot running outside in 2018

otherwise), Professor Sreenath's lab has been working on legged robots (the Cassie robot) with wheels at the bottom of each leg. This poses interesting control problems where standard bipedal robot balancing controllers fail after only a few seconds.

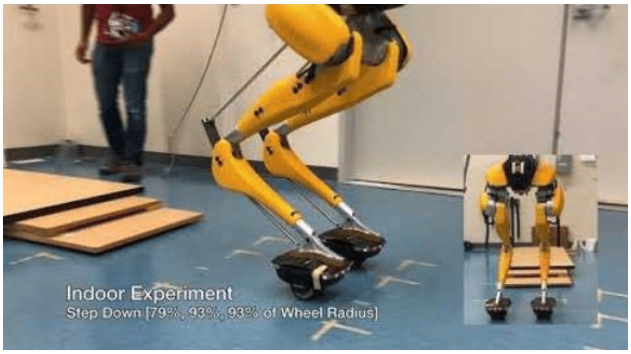

Figure 25.4: Cassie 2019 going down stairs while on hover shoes

25.3.1 Cassie Juggling

Dynamical model of ball:

$$m_b \ddot{x_b} = -m_b g e_3 + R f_b \tag{25.1}$$

Where m_b = mass of ball, x_b = position of ball, g = gravity, and f_b = contact force.

Dynamics of paddle:

$$m_p \ddot{x_p} = -m_p g e_3 - R f_b + f \tag{25.2}$$

$$J_p \dot{\Omega} = -\Omega \times J_p \Omega - R^T (x_b - x_p) \times f_b + M \tag{25.3}$$

Where m_p = mass of paddle, x_p = mass of paddle, and f, M are control inputs on the paddle.

Putting the paddle and Cassie together, the dynamics of the paddle become

$$D(q)\ddot{q} + H(q, \dot{q}) = Bu + J_s^T(q)\tau_s + J_c^T f_{feet} + J_b^T(q) f_b \tag{25.4}$$

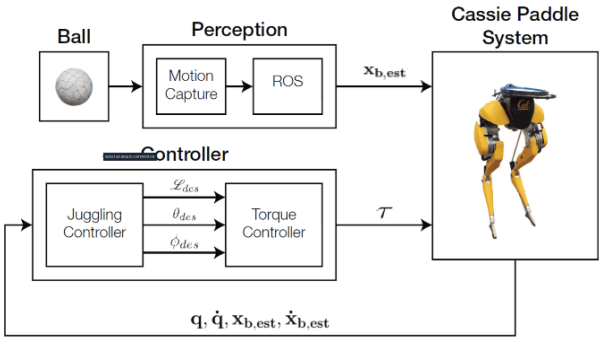

Figure 25.5: Feedback controller block diagram for Cassie juggling.

25.4 Dynamical Model of Ball Bouncing

The dynamics of a ball in free fall are

$$m\ddot{y} = -mg \tag{25.5}$$

where m is the mass of the ball, y is its position, and g is gravity.

When the ball y hits 0 (on 'impact'), the dynamics change. Therefore the ball bouncing model becomes

$$\begin{cases} m\ddot{y} = -mg, & y > 0 \\ \begin{bmatrix} y^+ \\ \dot{y}^+ \end{bmatrix} = \Delta(\begin{bmatrix} y^- \\ \dot{y}^- \end{bmatrix}), & y = 0 \end{cases} \tag{25.6}$$

where Δ is the impact map that maps state before impact to state after impact. There are several options for how this can be implemented depending on how sophisticated the model needs to be.

A simple model of the impact map for a bouncing model would be to set $y^+ = 0$ and $\dot{y^+} = -\eta\dot{y^-}$ where η is the coefficient of restitution. A more in sophisticated model might model the ground as a spring and damper to represent how impacts occur over milliseconds with continuous dynamics.

25.5 Dynamics of Legged Robot

25.5.1 Continuous Time Model

With the Lagrangian as $\mathcal{L}(q, \dot{q}) := K(q, \dot{q}) - V(q)$ and the Euler-Lagrange equations as $\frac{d}{dt}\frac{\partial \mathcal{L}}{\partial \dot{q}} - \frac{\partial \mathcal{L}}{\partial q} = \Gamma$, the legged robot continuous dynamics are

$$D(q)\ddot{q} + C(q,\dot{q})\dot{q} + G(q) = \Gamma \tag{25.7}$$

$$K(q,\dot{q}) = \frac{1}{2}\dot{q}'D(q)\dot{q} \tag{25.8}$$

$$C_{kj} = \sum_{i=1}^{N} \frac{1}{2}\left(\frac{\partial D_{kj}}{\partial q_i} + \frac{\partial D_{ki}}{\partial q_j} - \frac{\partial D_{ij}}{\partial q_k}\right)\dot{q}_i \tag{25.9}$$

$$G(q) = \frac{\partial V(q)}{\partial q} \tag{25.10}$$

The generalized force at a point is $\Gamma_i = \left(\frac{\partial p_i}{\partial q_i}\right)' F$.

25.5.2 Impact Model

Like in the bouncing ball case, the impact model is

$$x^+ = \Delta(x^-) \tag{25.11}$$

x^+ = state immediately after impact.

x^- = state immediately before impact.

Δ = impact map.

In the case of legged robots, some assumptions about the impact model include

- An impact results from contact of the swing leg end with the ground;
- the impact is instantaneous;
- the impact results in no rebound and no slipping of the swing leg;
- in the case of walking, at the moment of impact, the stance leg lifts from the ground without interaction, while in the case of running, at the moment of impact, the former stance leg is not in contact with the ground;
- the externally applied forces during the impact can be represented by impulses;
- the actuators cannot generate impulses and hence can be ignored during impact; and
- the impulsive forces may result in an instantaneous change in the robot's velocities, but there is no instantaneous change in the configuration.

As with the bouncing ball, there are various impact models which can be used. One is where $x^- = \begin{bmatrix} q^- \\ \dot{q}^- \end{bmatrix}$, $x^+ = \begin{bmatrix} q^+ \\ \dot{q}^+ \end{bmatrix}$, and $D(q)\ddot{q} + C(q,\dot{q})\dot{q} + G(q) = \Gamma + \delta F_{ext}$. Integrating this over the time of impact from t^- to t^+ gives $D(q^+)\dot{q}^+ - D(q^-)\dot{q}^- = F_{ext}$ where $F_{ext} = \int_{t^-}^{t^+} \delta F_{ext}(\tau)\mathrm{d}\tau$. The constraint corresponding to this is $J_{sw}(q^+)\dot{q}^+ = 0$.

25.5.3 Hybrid Model

Combining the continuous model and impact model gives a hybrid model, which can be depicted as in Figure 25.6.

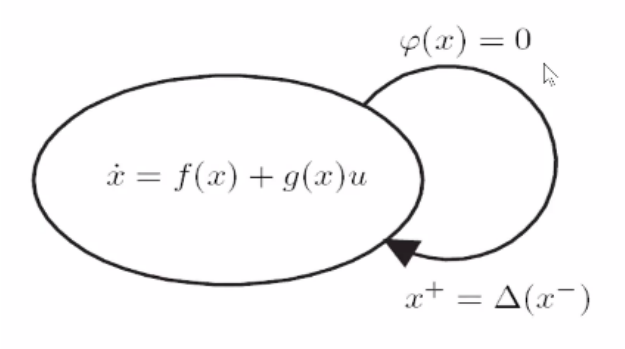

Figure 25.6: Continuos model combined with impact model

This can be further extended to a running robot as in Figure 25.7.

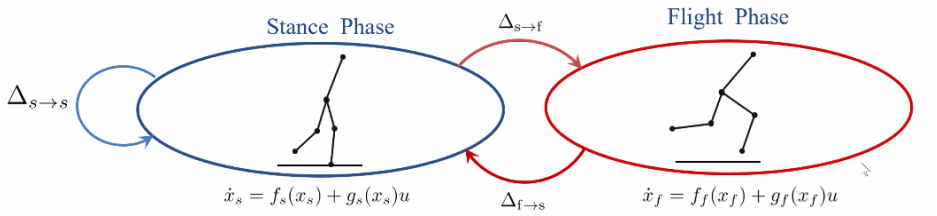

Figure 25.7: Continuos model combined with impact model for running robot

25.6 Simple Controllers

25.6.1 Zero Moment Point

Zero moment point walker only uses flat footed stage of Figure 25.8. To do this, the Center of Pressure (CoP) or Zero Moment Point (ZMP) must be kept within support polygon to maintain flat-footedness.

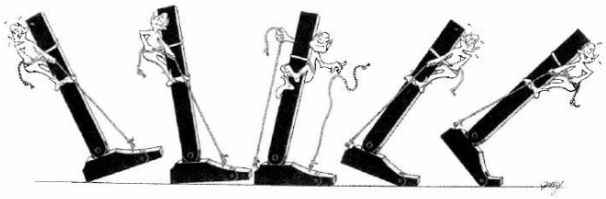

Figure 25.8: Foot position with respect to floor in various stages of walking.

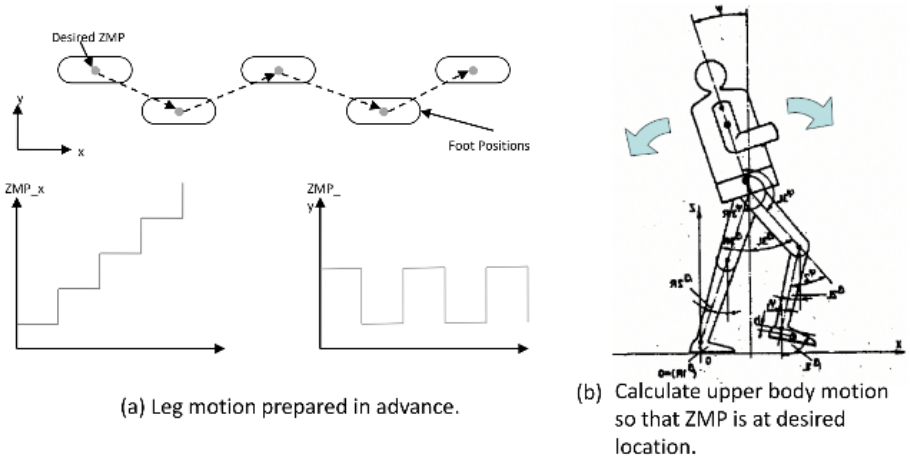

Figure 25.9: Movement of zero motion point during walking.

25.6.2 Raibert Controller

The Raibert controller for hopping robots used dynamic heuristics to produce walking motion.

Hopping height: $\tau_{spring} = k_p(h_{des}^{max} - h_{k-1}^{max})$

Body attitude: $\tau_{hip} = k_p(\phi_{des} - \phi) + k_v(\dot{\phi_{des}} - \dot{\phi})$

Hopping speed: regulate by foot placement (shorter step gives faster hopping speed). $x_f = \frac{\dot{x}T_s}{2} + k_{\dot{x}}(\dot{x} - \dot{x_{des}})$

A problem with heuristic controllers is they need a lot of tuning.

25.6.2.1 Bipedal Running

The Raibert controller can be extended to bipedal running since when running, only one leg is active at a time. This allows decomposition into a 'one-leg gait' where the 'idle leg' shortens the avoid ground contact while in air, extends to meet ground when needed, and the 'idle' role swaps between legs on liftoff of a leg.

25.6.2.2 Quadruped

The Raibert controller can be extended to multi-leg running by leveraging symmetry in legs. For quadrupeds, animal gaits use legs in pairs. This effectively reduces dimensionality, allowing legs to be coordinated together. See Figure 25.10 for three different gaits.

25.6.3 Passive Dynamic Walkers

Passive dynamic walkers are purely mechanical walkers which have no sensors, actuators, or power. As they lose energy to friction and on impacts, they often are designed to run on gentle slopes to regain energy. These tend to be extremely sensitive to initial conditions. The challenge in design of a passive walker is to design a mechanical system with a stable periodic orbit.

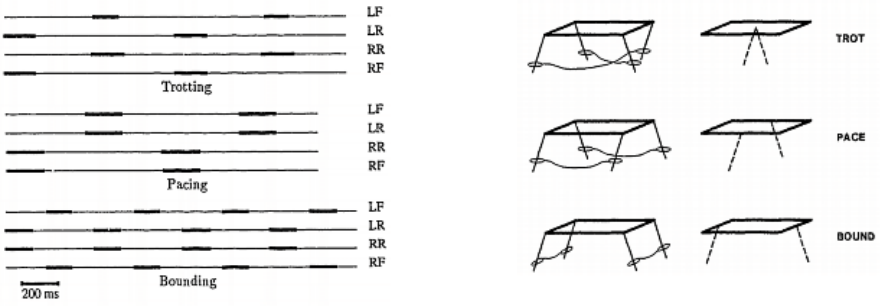

Figure 25.10: Various quadruped gaits.

The utility of passive walkers lies in their energy efficient design, which can be adapted to a powered walker design that uses significantly less energy than other walking robots.

25.6.3.1 Metrics of Efficiency

Two metrics of efficency are Specific Cost of Transport (CoT) and Specific Cost of Mechanical Transport (CmT).

Specific Cost of Transport is defined as

$$c_{et} = \frac{E}{Mgd} \tag{25.12}$$

Specific Cost of Mechanical Transport is defined as

$$c_{mt} = \frac{\int_0^T \sum_{i=1}^4 E_i(t)dt}{Mgd} \tag{25.13}$$

$$E_i(t) = \begin{cases} u_i(t)\dot{q}_i(t), & u_i(t)\dot{q}_i(t) > 0 \\ 0, & \text{else} \end{cases} \tag{25.14}$$

See Figure 25.11 for comparison of efficiencies of various bipedal robts, and a human. The passive robot performs better than a human, while passive-based robots are quite efficent as well.

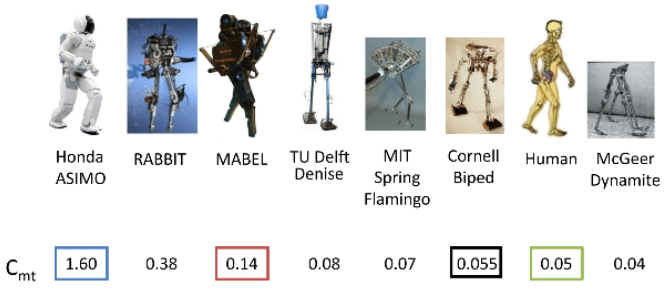

Figure 25.11: Specific Cost of Mechanical Transport comparing various machines.